Transmembrane Interactions in the Activation of the Neu Receptor Tyrosine Kinase†

Steven O. Smith,*,‡ Charles Smith,§ Srinivasan Shekar,‡,§ Olve Peersen,§,|| Martine Ziliox,‡ and Saburo Aimoto⊥

Department of Biochemistry and Cell Biology, Center for Structural Biology, SUNY Stony Brook, Stony Brook, New York 11794-5115, Department of Molecular Biophysics and Biochemistry, Yale University, New Haven, Connecticut 06520, and Institute for Protein Research, Osaka University, Osaka, Japan

Received December 4, 2001

ABSTRACT: The Neu receptor tyrosine kinase is constitutively activated by a single amino acid change in the transmembrane domain of the receptor. The mutation of Val664 to glutamate or glutamine induces receptor dimerization and autophosphorylation of the receptor's intracellular kinase domain. The ability of this single mutation to activate the receptor is sequence-dependent, suggesting that specific helix−helix interactions stabilize the transmembrane dimer. We have determined the local secondary structure and interhelical contacts in the region of position 664 in peptide models of the activated receptor using solid-state rotational resonance and rotational echo double-resonance (REDOR) NMR methods. Intrahelical ^{13}C rotational resonance distance measurements were made between 1-^{13}C-Thr662 and 2-^{13}C-Gly665 on peptides corresponding to the wild-type Neu and activated Neu* transmembrane sequences containing valine and glutamate at position 664, respectively. We observed similar internuclear distances (4.5 ± 0.2 Å) in both Neu and Neu*, indicating that the region near residue 664 is helical and is not influenced by mutation. Interhelical $^{15}N\cdots^{13}C$ REDOR measurements between Gln664 side chains on opposing helices were not consistent with hydrogen bonding between the side chain functional groups. However, interhelical rotational resonance measurements between 1-^{13}C-Glu664 and 2-^{13}C-Gly665 and between 1-^{13}C-Gly665 and 2-^{13}C-Gly665 demonstrated close contacts (4.3−4.5 Å) consistent with the packing of Gly665 in the Neu* dimer interface. These measurements provide structural constraints for modeling the transmembrane dimer and define the rotational orientation of the transmembrane helices in the activated receptor.

Receptor tyrosine kinases (RTKs) are integral membrane proteins containing a large extracellular ligand-binding domain, a single transmembrane helix, and a large intracellular kinase domain. The binding of peptide growth factors to the extracellular domain of the receptor triggers the dimerization of receptor monomers or a change in the relative orientation of monomers in preformed receptor dimers (*1*−*3*). Ligand binding leads to the autophosphorylation of tyrosine residues in the intracellular kinase domain. Many of the molecular details concerning the mechanism of receptor activation have emerged from crystal structures of the extracellular ligand binding domain and the intracellular tyrosine kinase domain of RTKs and related receptors (*4*). Much less is known about how the transmembrane domain of RTKs may function to couple ligand binding to tyrosine phosphorylation.

The Neu RTK provides the most direct evidence that specific interactions between transmembrane helices can mediate dimerization and receptor activation (*5*). Bargmann and Weinberg found that a single amino acid in the transmembrane domain (Val664) when changed to glutamic acid causes constitutive activation of the Neu receptor (*6*−*8*). Replacement with other amino acids showed that the substitution was specific to glutamate and glutamine. Stern and co-workers found that this V664E substitution induces receptor dimerization and that the position of the glutamate in the transmembrane sequence was important (*9*). The ability of this substitution to activate the receptor was disrupted if a three-amino-acid sequence containing the glutamate (VEG) was shifted by one residue toward the N-terminus or by eight residues (corresponding to two helical turns) toward the C-terminus of the receptor. These results indicated that the relative orientations of the transmembrane helices and the kinase domains are critical for receptor activation. More recently, Donoghue and co-workers (*10*) extended these studies by showing that the transmembrane and kinase domains are "rotationally coupled". They observed a helical periodicity in the ability of transmembrane glutamates to activate the Neu receptor.

The ability of the V664E substitution to confer constitutive activation is not limited to the Neu receptor. Substitution of the transmembrane domain of the activated Neu* receptor into several other RTKs can cause constitutive activation,

† This work was supported by the National Institutes of Health under Grant No. GM-46732 and by the National Science Foundation under Instrumentation Grant No. 9907840.

* Corresponding author. Telephone: 631-632-1210. Telefax: 631-632-8575. E-mail: steven.o.smith@sunysb.edu.

‡ SUNY Stony Brook.

§ Yale University

|| Present address: Department of Biochemistry and Molecular Biology, 316 Molecular and Radiological Biosciences Bldg., Colorado State University, Ft. Collins, CO 80523.

⊥ Institute for Protein Research, Osaka University.

[1] Abbreviations: CPMG, Carr Purcell Meiboom Gill; POPC, palmitoleoylphosphocholine; POPS, palmitoleoylphosphoserine; MAS, magic-angle spinning; NMR, nuclear magnetic resonance; REDOR, rotational echo double resonance; RR, rotational resonance; RTK, receptor tyrosine kinase; TOXCAT, ToxR chloramphenicol acetyltransferase; TM, transmembrane.

10.1021/bi012117l CCC: $22.00
Published on Web 07/02/2002

autophosphorylation, and cell transformation (*11*−*13*). Even in the case of the insulin receptor, which exists as a disulfide-linked dimer, substitution of the activated Neu* receptor transmembrane domain leads to receptor activation (*12*). These studies have supported the idea that the transmembrane helices in RTKs adopt a specific orientation upon ligand-induced dimerization and that the V664E mutation locks the transmembrane helices in the "active" orientation in the absence of ligand.

The best evidence for transmembrane interactions in wild-type RTKs comes from the observation that truncation of the extracellular domain often leads to constitutively active receptor dimers (*14*−*19*). In this regard, Sternberg and Gullick identified a sequence motif that occurs frequently in the transmembrane domains of RTKs (*20*). The motif has a proline residue in the extracellular juxtamembrane region, a relatively well-conserved sequence (AXXVG) in the transmembrane domain that is followed by a sequence rich in leucines, valines, and isoleucines. They proposed that this motif is associated with receptor dimerization and were able to show that peptides containing this sequence inhibited transformation of cells containing the activated Neu* receptor (*21*). These studies indicate that transmembrane Neu peptides can independently fold in membranes and interact with the full-length receptor, thus setting the stage for structural studies on the transmembrane domain alone.

The rotational orientation of the transmembrane helices in the activated Neu* receptor appears to be roughly defined by the position of the glutamic acid or glutamine residue at position 664. Burke and Stern (*22*) proposed a detailed model of the dimer interface based on the ability of cysteine substitutions in the juxtamembrane region to form active disulfide-linked receptors. They observed that receptor activation is most strongly induced by cysteine substitutions at Val656 and Thr657. These residues fall on the same face as Val664 (or Glu664 in Neu*) in the helical dimer which they modeled as a left-handed coiled coil of helices extending from the juxtamembrane region through the transmembrane domain of the receptor.

Despite extensive mutational studies on the Neu and Neu* receptors, there are still open questions concerning the specific residues that form the dimer interface and the correct rotational orientation of the transmembrane helices needed for receptor activation. For instance, the dimer interface proposed by Burke and Stern (*22*) on the basis of cross-linking data does not include Gly665 of the VEG and AXXVG motifs previously thought to be essential for dimerization. Furthermore, molecular dynamics simulations suggest that there are local distortions in the transmembrane helix in the region of residue 664 and that the active dimer may actually be nonsymmetric (*23*).

Solid-state NMR using magic-angle spinning provides a way to establish which amino acids lie in the helical interface of the activated Neu* transmembrane dimer. A key advantage of solid-state NMR approaches is that the measurements can be made in membrane bilayers. Magic-angle spinning (MAS) yields high-resolution spectra of proteins with restricted motion (*24*). Importantly, in the past 10 years, a wide range of MAS methods have been developed for measuring weak dipolar couplings (*25*, *26*). These couplings can be directly related to internuclear distances. We have previously shown that the peptides corresponding to the activated Neu* transmembrane domain can be reconstituted into bilayers for structural studies (*27*, *28*). MAS NMR measurements demonstrated that Glu664 is protonated due to the high surface pH and is strongly hydrogen bonded (*27*). The observation of a narrow well-resolved resonance for the 5-^{13}C-Glu664 carboxyl group with an unusual downfield chemical shift suggested that the hydrophobic Neu* peptides tightly associate in membrane bilayers (*27*).

In this paper, we use rotational resonance (*29*, *30*) and REDOR (*31*) methods for measuring both intramolecular and intermolecular distances in wild-type Neu and activated Neu* peptides. The strategy is to first establish the local secondary structure near Val664 in the wild-type peptide and near Glu664 in peptides containing the activating mutation. Previous FTIR measurements have shown that the global secondary structure of the Neu* transmembrane sequence is α-helical (*27*), while rotational resonance NMR measurements have shown that the local secondary structure is helical between positions 665 and 669 in the wild-type Neu and activated Neu* peptides (*28*). However, local distortions between Thr662 and Gly665 are not ruled out by these data. In particular, two sequential valines in the wild-type sequence (Val663 and Val664) are thought to induce a π-bulge (*23*).

Once the local secondary structure is established, dimer contacts can be established by measuring dipolar couplings between ^{13}C- and ^{15}N-labeled sites across the dimer interface. A few selective high-resolution distances derived from intermolecular dipolar couplings provide tight constraints for defining the rotational orientation of the transmembrane helices in the Neu* dimer. Here, we address whether hydrogen bonding interactions between the side chains of Gln664 stabilize the helix dimer as previously proposed (*27*) and determine whether Gly665, long thought to be part of the dimerization motif, lies in the dimer interface.

MATERIALS AND METHODS

The lipids (Avanti Polar Lipids, Alabaster, AL) used were palmitoleoyl phosphatidylcholine (POPC) and palmitoleoyl phosphatidylserine (POPS). The isotopically labeled amino acids were obtained from the following sources: 1-^{13}C-threonine, Cambridge Isotope Labs (Andover, MA); 1-^{13}C-glycine and 2-^{13}C-glycine, Mass Trace (Woburn, MA); and 1,5-^{13}C-glutamate, Stable Isotope Resource at Los Alamos Laboratory.

Synthesis and Reconstitution of Neu Transmembrane Peptides. The transmembrane sequence of Neu corresponding to residues 649−686 was synthesized using solid-phase methods (*27*, *28*). The residue at position 664 was valine (Neu), glutamine (Neu*), or glutamate (Neu*).

AEQRASPVTFIIATV-X_{664}-GVLLFLALVVVVGILIKR-RRYK

Purification of the crude peptide by reverse-phase high-performance liquid chromatography (HPLC) was as follows. Crude peptide (~5 mg) was dissolved in 1 mL of trifluoroacetic acid, injected onto a reverse phase C4 or C18 HPLC column, and purified by gradient elution using distilled (Millipore) water (solvent A), 95% acetonitrile (solvent B), and 95% 2-propanol (solvent C). The initial aqueous solvent conditions (80% A, 9% B, 11% C) were first changed to a more hydrophobic composition (25% A, 30% B, 45% C) in a single step, and then a linear gradient was applied to

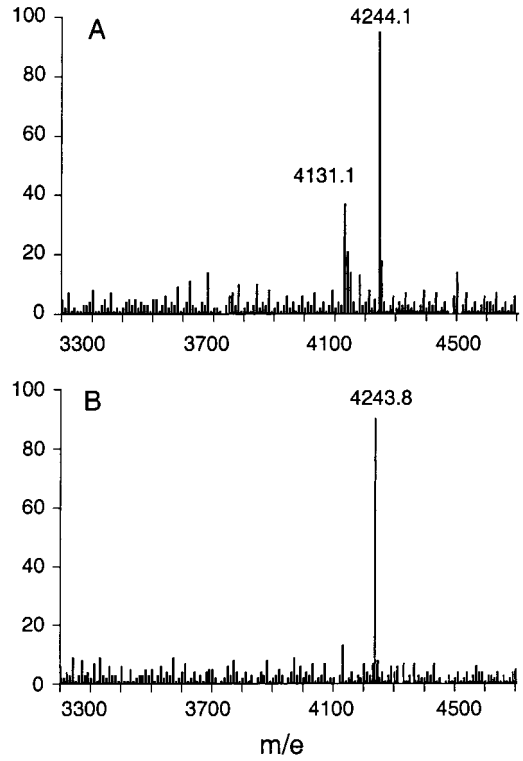

FIGURE 1: Mass spectra of the crude (a) and HPLC-purified (b) Neu* transmembrane peptide. The molecular ion is at 4244 *m*/*e*. The peak at 4131 *m*/*e* in the crude peptide is removed by reverse-phase HPLC.

gradually change the solvent composition to 18% A, 33% B, and 49% C, where the peptides elute. The elution was monitored by the optical absorbance at 280 nm. The solutions corresponding to the peaks were collected into several fractions. The fractions were then lyophilized and checked by mass spectrometry for purity. Figure 1 shows the mass spectrum of the crude Neu* peptide (a) and the mass spectrum of the HPLC fraction containing the pure peptide (b). These spectra illustrate the ability to separate peptides with a molecular weight of ~110 kDa less than the molecular ion.

The peptides were reconstituted into POPC:POPS multilamellar dispersions by detergent dialysis. The reconstitution protocol is similar to that established for reconstitution of the transmembrane domain of glycophorin A, which is known to dimerize in membrane bilayers (*32*, *34*). Octyl β-glucoside was used for the detergent because of its high critical micelle concentration. The lipid (POPC and POPS), peptide, and detergent (octyl β-glucoside) were dissolved in trifluoroethanol. The lipid-to-protein molar ratio was 30:1, and the POPS was 14% of the total lipid by weight. The intermolecular REDOR and rotational resonances measurements required that peptides with different isotopic labels be co-mixed during the reconstitution. For the REDOR experiments, we used a 1:1 molar ratio, which results in 50% of the peptides associating as ^{13}C:^{15}N heterodimers. For the rotational resonance experiments, a 4:1 ratio of labeled peptides was used.

Following cosolubilization, the trifluoroethanol solution was removed by vacuum, and the dry lipid/peptide/detergent mixture was rehydrated with phosphate buffer (10 mM phosphate and 50 mM NaCl, pH 7), such that the final concentration of octyl β-glucoside was 5% (w/v). The rehydrated sample was stirred slowly for at least 6 h, and then the octyl β-glucoside was dialyzed using Spectra-Por dialysis tubing (3500 MW cutoff) for 24 h against phosphate buffer at a temperature above the lipid phase transition. The dialysis solution was changed several times. Sucrose gradient (10%-40% w/v) ultracentrifugation at 150 000 *g* for 8−12 h at 15 °C was used to isolate homogeneous lipid vesicles. As with the glycophorin A transmembrane peptide, the reconstituted membranes form two discrete bands in the sucrose gradient (*34*). The upper band has a more homogeneous appearance and a higher lipid:peptide ratio (40:1−60:1) as assessed by FTIR analysis. The lower band has an aggregated appearance and a lower lipid:peptide ratio (10:1−30:1). The sucrose in each band was dialyzed against phosphate buffer for 24 h. Following dialysis, the reconstituted membranes were incubated at 35−40 °C for up to 96 h.

FTIR Spectroscopy. Polarized ATR-FTIR spectra were collected on a Nicolet Magna 550 spectrometer as previously described (*27*). The frequency and dichroic ratio of the amide I vibration provide information on the secondary structure and orientation of the reconstituted peptides. The measurements were made on reconstituted membranes that have been layered on a germanium ATR plate with a film thickness of greater than ~10 μm. As a result, we used the thick film approximation (*33*) to translate the observed dichroic ratios into helix orientation since the film thickness is much greater than the penetration depth (~1 mm) of the evanescent wave. The analysis is similar to that previously described (*27*), except that the angle α between the helix director and the transition dipole moment of the amide I vibrational mode is set to 41.8° on the basis of parallel experiments on bacteriorhodopsin. A complete description of our FTIR experimental setup and analysis has recently been described for structural studies on the transmembrane dimer of glycophorin A (*34*).

NMR Spectroscopy. Magic-angle spinning NMR experiments were performed at 360 MHz on a Chemagnetics CMX spectrometer using 5 mm rotors and at 400 MHz on a Bruker DMX spectrometer using 4 mm rotors. ^{15}N-observe REDOR and ^{13}C-observe rotational resonance spectra were acquired with ramped amplitude cross polarization (*35*) and two-pulse phase-modulation proton decoupling during acquisition (*36*). The ^{1}H, ^{13}C, and ^{15}N pulse lengths were typically 3.5, 4, and 5 μs, respectively. The total contact time for cross polarization was 3 ms ,and the recycle delay was 2.5 s. Proton decoupling field strengths were generally higher than ~75 kHz on the 360 MHz spectrometer used for the rotational resonance experiments and ~90 kHz on the 400 MHz spectrometer used for the REDOR experiments. Signals were averaged in blocks of 1024 or 2048 transients. The time domain signals were zero filled to 2048 or 4096 points and multiplied by a 10−20 Hz line broadening function before Fourier transformation. Sample spinning speed was generally kept constant to within 5 Hz. The ^{15}N chemical shifts are referenced to 5.6 M $^{15}NH_4Cl$ (0.0 ppm), which is 15.4 ppm downfield from solid $^{15}NH_4Cl$. The ^{13}C frequencies were referenced to the carbonyl resonance of solid glycine at 176.02 ppm from TMS. The sample temperature was maintained at −10 °C.

The experimental design of the rotational resonance experiment has been described previously (*30*). The sequence

begins with $^{1}H-^{13}C$ cross polarization to generate ^{13}C polarization, which is then stored on the *Z* axis with a ^{13}C flip-back pulse. The $^{13}C{=}O$ or $^{13}CH_2$ resonance is selectively inverted with a low-power 500 μs pulse, and magnetization is allowed to exchange between the two ^{13}C-labeled sites for a variable mixing period (t_m). The power level of the inversion pulse is carefully adjusted to yield the maximum inversion. The distribution of ^{13}C signal at the end of the mix period is detected with a 90° pulse that flips the magnetization into the transverse plane for acquisition of the NMR signal. For the intrahelical rotational resonance measurements, we integrated the intensities of both the $^{13}C{=}O$ or $^{13}CH_2$ resonances. For interhelical measurements, only the intensity of the noninverted resonance, which is well resolved and requires minimal correction (see below), was integrated. The analysis of the intensity change of a single resonance is identical to the analysis used for the intrahelical measurements where the difference in the integrated intensities of the two dipole coupled resonances is plotted as a function of the rotational resonance exchange time. The only drawback to analyzing the decay of just the noninverted resonance in an interhelical measurement is sensitivity. For these experiments, it is important to incorporate ramped amplitude cross polarization in order to obtain stable, quantitative intensities of the $^{13}C{=}O$ and $^{13}CH_2$ resonances (*37*).

Simulations were carried out using the program cc2Z (*38*) written by M. Levitt (Stockholm, Sweden). The anisotropy and asymmetry parameters for the carbonyl (10630 Hz, 0.85), methyl (1672 Hz, 0.32), and methylene carbons (1510 Hz, 0.95) were taken from the literature (*30*). The value of the zero quantum T_2 relaxation time (1.4 ms) used in the simulations was based on glycophorin A peptides bearing a $^{13}CH_2{\cdots}^{13}C{=}O$ spin pair at a known intramolecular distance (*32*). The hydrophobic glycophorin A transmembrane sequence has approximately the same length as the transmembrane domain of the Neu receptor, forms dimers in membranes, and exhibits roughly the same 2 ppm line widths. In intramolecular rotational resonance measurements on the Neu peptide labeled at 1-^{13}C-Thr662 and 2-^{13}C-Gly665, a 1.4 ms zero-quantum T_2 yields a 4.5 Å distance (see Results). The 1-$^{13}C{\cdots}$2-^{13}C distance in this case is predicted to be 4.5 Å if the Neu sequence is α-helical. The problem with using the Neu intrahelical measurement as an internal standard is that we do not independently know that the Neu peptides are helical in the region being probed. However, these measurements set the lower limit of the zero-quantum T_2 since a smaller value would predict an unrealistically short distance. The upper limit of the zero quantum T_2 is set by studies on crystalline model compounds and by the homogeneous T_2 measured with a CPMG echo sequence. Rotational resonance measurements of a known $^{13}C{=}O$ carbonyl to $^{13}CH_2$ methylene distance in the microcrystalline model tripeptide AGG yield an estimate of the zero-quantum T_2 of 2 ms (M. Eilers and S. O. Smith, unpublished results), while the CPMG measurement yields a homogeneous T_2 of 1.8−1.9 ms. The uncertainty in the zero quantum T_2 parameter (1.4−2 ms) corresponds to an error of ±0.2 Å for a 4.5 Å distance measurement.

The experimental rotational resonance data were corrected to account for the amount of decay observed in off-rotational resonance experiments. The data were also corrected to account for the fact that the peptides with different ^{13}C labels were mixed in a 4:1 ratio to form "heterodimers". This correction is necessary because homodimers (with the same ^{13}C labels) form along with the desired heterodimers, and only the heterodimers contribute to rotational resonance exchange. With a 4:1 ratio, the contribution of ^{13}C signal from the homodimer is 29%.

The REDOR pulse sequence uses a train of ^{13}C π pulses with two pulses per rotor cycle. XY8 phase cycling was used to suppress resonance offset effects (*39*). A single ^{15}N π pulse was used to refocus the chemical shift interaction. REDOR experiments were carried out with 48 and 64 rotor cycles of dephasing pulses. Acquisition of the full S_o and dephased S spectra were interleaved to help compensate for long-term spectrometer drift. The normalized echo differences, $\Delta S/S_o$, for these two experiments were analyzed using a Mathematica program kindly provided by Terry Gullion (Mississippi State University). The dipolar coupling in turn is related to the internuclear distance by the equation $D = \gamma_1\gamma_2 h/2\pi r^3$, where γ_1 and γ_2 are the gyromagnetic ratios of the coupled ^{13}C and ^{15}N spins, h is Planck's constant, and r is the internuclear distance. The calculated $^{15}N{\cdots}^{13}C$ dipolar couplings accounted for reconstitution of the ^{15}N- and ^{13}C-labeled peptides in a 1:1 ratio.

Molecular Dynamics Simulations and Energy Minimization. The computational search strategy using the program CHI has been described previously by Adams et al. (*40*, *41*). Low-energy conformations of helix dimers were searched by rotating each helix through rotation angles $\varphi 1$ and $\varphi 2$ from 0 to 360° with a sampling size of 45°. The starting geometry included both left-handed and right-handed crossing angles. Four different runs were carried out for each starting geometry using simulated annealing of all atomic coordinates. The rotation and crossing angles were allowed to vary. The results of the search can be shown on a grid of $\varphi 1$ and $\varphi 2$. The initial grid exhibits points equally separated by 45°. The final minimized structures, however, migrate from their initial geometry and often "cluster" in low-energy wells. The individual structures in each low-energy cluster are averaged and reminimized. The resulting averaged structure from each cluster is then evaluated on the basis of the NMR distance measurements and mutational data in the literature. The structures with left-handed and right-handed crossing angles which best explain the NMR and mutational results are then reminimized using the NMR distances as constraints.

RESULTS AND DISCUSSION

Neu and Neu Transmembrane Domains Are Helical in the Region of Residue 664.* The first series of experiments that were undertaken were designed to establish the local secondary structure near Val664 in the wild-type Neu peptide and near Glu664 in the activated Neu* peptide. We have previously shown using polarized IR spectroscopy that peptides corresponding to the transmembrane domain of the activated Neu* receptor can be reconstituted into lipid bilayers in a helical transmembrane orientation (*27*). However, the polarized IR measurements are not extremely sensitive to local changes in helical structure. Molecular dynamics simulations have suggested that the helical secondary structure near position 664 may be distorted (*23*, *42*).

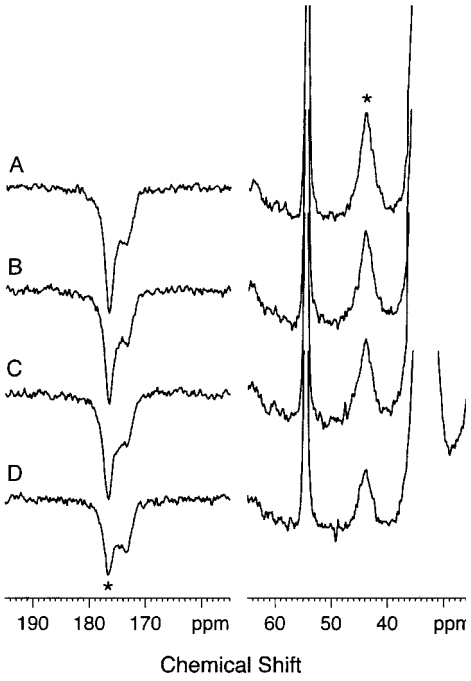

FIGURE 2: Intramolecular ^{13}C rotational resonance NMR spectra of the Neu* transmembrane peptide labeled at 1-^{13}C-Thr662 and 2-^{13}C-Gly665. The carbonyl resonance of 1-^{13}C-Gly665 was inverted, and spectra were obtained with exchange times of 100 μs (A), 5 ms (B), 10 ms (C), and 30 ms (D). The MAS frequency was maintained at 11.764 kHz $\pm$ 5 Hz, corresponding to the $n = 1$ resonance condition.

For example, Brandt-Rauf et al. (*42*) found that the global minimum-energy conformation of the Neu receptor contained a sharp bend at positions 664 and 665, while the transmembrane sequence of Neu* existed as an α-helix. In their simulations, Sajot and Genest (*23*) often observed local π distortions in the helical backbone, which they attributed in most cases to consecutive Val residues. The π distortions result in the exclusion of a carbonyl group from the backbone hydrogen bonding network.

We previously demonstrated using rotational resonance NMR that there is no significant difference in helical secondary structure between residues 665 and 669 in the Neu and Neu* transmembrane peptides (*28*). These sites span the helical turn just below residue 664. To address the local secondary structure in the region of residue 664, we used rotational resonance NMR to measure the intramolecular distance between Thr662 and Gly665 in the Neu and Neu* sequences. Figure 2 presents intrahelical ^{13}C rotational resonance spectra obtained of the Neu* transmembrane peptide labeled with 1-^{13}C-Thr662 and 2-^{13}C-Gly665. The MAS frequency was set at 11 764 Hz $\pm$ 5 Hz, which corresponds to the chemical shift difference between the two dipole-coupled spins. The carbonyl resonance of 1-^{13}C-Thr662 at ~176 ppm was inverted, and spectra were obtained with mixing times between 100 μs (a) and 30 ms (d). With increasing mixing time, the Thr662 carbonyl resonance becomes less negative, and Gly665 α-carbon becomes less positive as magnetization is exchanged. The other resonances (e.g., the lipid carbonyl at ~173 ppm) do not change significantly in intensity.

The distance between the ^{13}C labels in the Neu and Neu* peptides is sensitive to the intervening secondary structure. The distance would be ~4.5 Å in a canonical helix with i to $i + 4$ hydrogen bonding and greater than 9 Å in extended β-structure. In a helix containing a π-bulge and i to $i + 5$ hydrogen bonding, the corresponding distance can be greater than 5.5 Å. For instance, in helix G of bacteriorhodopsin (Protein Data Bank access code 1C3W), there is a π-bulge at Ala215, and the distance between the carbonyl carbon of Ala215 and the α-carbon of Gly218 is 5.6 Å.

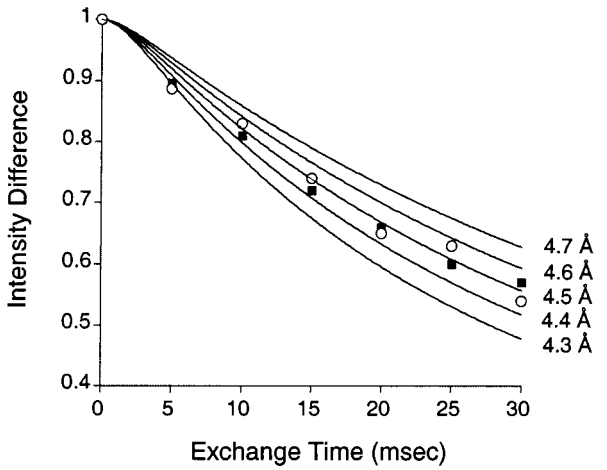

FIGURE 3: Intramolecular ^{13}C rotational resonance magnetization exchange curves and simulations. Experimental data are shown for the [1-^{13}C-Thr662, 2-^{13}C-Gly665] Neu (open circles) and Neu* (filled squares) transmembrane peptides reconstituted into POPC. POPS:POPS multilayers. In a canonical helix, the ^{13}C-labels are separated by ~4.5 Å. Simulations of the magnetization exchange are shown with solid lines for internuclear distances between 4.3 and 4.7 Å using a zero quantum T_2 relaxation time of 1.4 ms.

The intensity changes in the coupled ^{13}C resonances are translated into an internuclear distance by first plotting the average difference intensity $\langle ^{13}CH_2—^{13}C{=}O\rangle$ as a function of the exchange time. Figure 3 presents the experimental magnetization exchange curves of the [1-^{13}C-Thr662, 2-^{13}C-Gly665] Neu (open circles) and Neu* (filled squares) transmembrane peptides. Within experimental error, the Thr662-Gly665 distance is the same in the Neu and Neu* structures. These data argue against a difference in local secondary structure (i.e., a distortion or kink) between the wild-type and activated Neu* sequences. Simulations of the magnetization exchange are shown with solid lines for internuclear distances of 4.3−4.7 Å. The experimental data are best fit by the 4.5 Å simulations, consistent with α-helical secondary structure. The precision of the measurements, as reflected in the scatter of points relative to the simulated curves, is on the order of $\pm$ 0.1 Å. The accuracy in the measurements is generally worse than the precision (*30*) and is estimated to be on the order of $\pm$0.2 Å on the basis of error in the position of the first data point in the exchange curves and error in the estimate of the zero-quantum T_2 (see Methods). Finally, in the modeled structure below, the interhelical distance between these labels is predicted to be ~7 Å, and consequently, interhelical couplings do not contribute to the intrahelical magnetization exhange.)

Do Gln664 Side Chains Hydrogen Bond across the Dimer Interface? MAS NMR studies on the activated Neu* receptor first revealed that the Glu664 carboxyl group was protonated and strongly hydrogen bonded (*27*). These studies were based on measurements of the ^{13}C chemical shift anisotropy of the Glu664 carboxyl group and led to models of the Neu* receptor dimer with the COOH side chains directly hydrogen

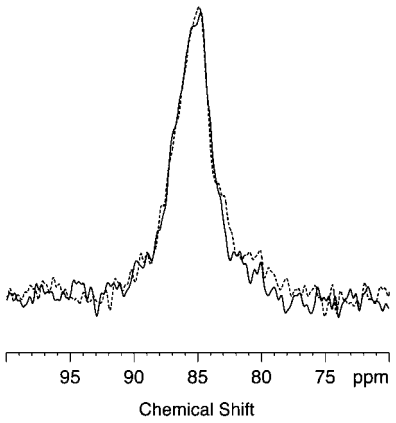

FIGURE 4: Interhelical ^{15}N-observe REDOR NMR measurements. Full So (solid curves) and reduced S (dotted lines) REDOR spectra of ^{15}N-Gln664 Neu* combined with 5-^{13}C-Gln644 Neu*. The reduced S spectra were obtained using 64 rotor cycles of ^{13}C dephasing pulses. Peptides reconstituted into POPC:POPS multilayers. Acquisition of the full So and reduced S spectra were interleaved to help compensate for long-term spectrometer drift.

bonded to one another. To test for direct side chain hydrogen bonding contacts, we synthesized Neu* transmembrane peptides with 5-^{13}C-Gln and 5-^{15}N-Gln at position 664. While both glutamate and glutamine are effective in activating the Neu receptor (*6*), the glutamine side chain has advantages for heteronuclear REDOR measurements since it can be labeled at either the amide $^{13}C{=}O$ or $^{15}NH_2$.

The ^{15}N-observe REDOR experiment requires the acquisition of two spectra, a full echo spectrum, S_o, with no dephasing pulses on the ^{13}C channel, and a reduced spectrum, S, resulting from the application of a ^{13}C train of dephasing pulses. In the REDOR experiments, the intensity change (ΔS) between the two spectra is related to the dipolar coupling and hence the internuclear distance. If the glutamine side chains are hydrogen bonded, we would predict a $^{13}C\cdots{}^{15}N$ distance of 4.0 $\pm$ 0.5 Å and intensity changes (ΔS) in the REDOR spectra of ~14% and 22% with 48 and 64 rotor cycles, respectively, at a MAS frequency of 4 kHz. Figure 4 presents the full (solid line) and reduced (dashed line) REDOR spectra of 5-^{15}N-Gln Neu* complexed with 5-^{13}C-Gln Neu* with 64 rotor cycles of dephasing pulses. Since the natural abundance of ^{15}N (0.37%) is significantly less than the natural abundance of ^{13}C (1.1%), the ^{15}N signal from the peptide backbone is small and easily subtracted from the ^{15}N spectrum. The lack of a significant change in the intensity of the 5-^{15}N-Gln resonance between the full S_o and reduced S REDOR spectra indicates that the Gln664 amide functional groups are not in close proximity and not strongly hydrogen bonded.

The absence of Gln−Gln interactions was surprising, particularly in light of recent studies showing that glutamine and glutamate can drive the nonspecific association of transmembrane peptides (*43*). To explore the possibility that Gln interactions may be nonspecific and lead to peptide aggregation, we also made REDOR measurements on the reconstituted Neu* peptides obtained from the lower bands in our sucrose gradients (see Methods section). In contrast to the measurements on the reconstituted peptides isolated from the upper bands, we observed a ~12% decrease in the 5-^{15}N-Gln664 resonance after 64 rotor cycles of ^{13}C dephasing pulses (data not shown). This corresponds to a dipolar coupling of ~32 Hz (after accounting for reconstitution of the ^{15}N- and ^{13}C-labeled peptides in a 1:1 ratio) and an average internuclear distance of ~4.5 Å. As discussed in more detail in our work on glycophorin A, the lower bands in sucrose gradients have lower lipid-to-peptide ratios and exhibit lower dichroic ratios in polarized FTIR measurements. The working hypothesis is that these bands contain aggregated peptide (*32*,*34*). These results are consistent with the activated Neu* peptides forming nonspecific aggregates in the lower bands on the sucrose gradients.

Gly665 Packs in the Neu Dimer Interface.* In the wild-type Neu sequence, Gly665 is part of a "AXXVG" motif common to the family of receptor tyrosine kinases and thought to facilitate transmembrane helix interactions (*20*). In the activated Neu* sequence, Gly665 is part of the VEG tripeptide that has been implicated in receptor dimerization and activation (*9*). The most direct evidence that Gly665 is important in mediating receptor dimerization comes from mutational studies of Neu* where replacement of Gly665 with valine disrupts dimerization and receptor activation (*44*). In this section, we explore possible interhelical glycine contacts using rotational resonance NMR. Recently, glycine has been shown to be important for mediating helix−helix interactions in both single pass (*32*) and polytopic membrane proteins (*45*).

Figure 5a presents interhelical rotational resonance magnetization exchange curves for 2-^{13}C-Gly665-labeled Neu* transmembrane peptides reconstituted with Neu* peptides labeled at 1-^{13}C-Gly665 (solid circles). These experiments are similar to the intrahelical rotational resonance experiments described above, except that the ^{13}C-labels are incorporated into separate peptides. 2-^{13}C-Gly665 Neu* peptides were reconstituted into membrane multilamellar dispersions in a 1:4 molar ratio with 1-^{13}C-Gly665 Neu* peptides. In these experiments, the 1-^{13}C-Gly resonance was inverted, and only the 2-^{13}C-Gly665 resonance was monitored to follow magnetization exchange. The 2-^{13}C Gly665 resonance is well resolved at 43 ppm in the MAS spectrum of Neu*, and the 1:4 dilution increases the fraction of the 2-^{13}C-Gly665 Neu* peptide that interacts with the 1-^{13}C-Gly665 Neu* peptide.

The experimental data (solid squares) for the interhelical Neu*−Neu* measurements are shown in Figure 5a along with a series of simulations based on distances from 4.3 to 4.7 Å. The intensity changes of the 2-^{13}C-Gly665 resonance correspond to an internuclear distance of 4.5 Å. These calculations assume that Neu* transmembrane helices dimerize quantitatively in a head-to-head fashion. The observation of significant magnetization exchange supports this assumption. Importantly, if there is a distribution of monomers and dimers in the reconstituted membranes, the actual internuclear distance in the dimer would be shorter than 4.5 Å since the observed decay curve would be the average of rapid magnetization exchange from the dimers and essentially no exchange from the monomers. Additional support for dimer interactions between transmembrane Neu and Neu* peptides comes from several sources. First, expression studies show that short peptide sequences corresponding to both the Neu and Neu* transmembrane domains are able to inhibit transformation in vitro and in vivo (*21*). Second, deuterium NMR studies on synthetic and expressed peptides corresponding to the Neu and Neu* transmembrane domains

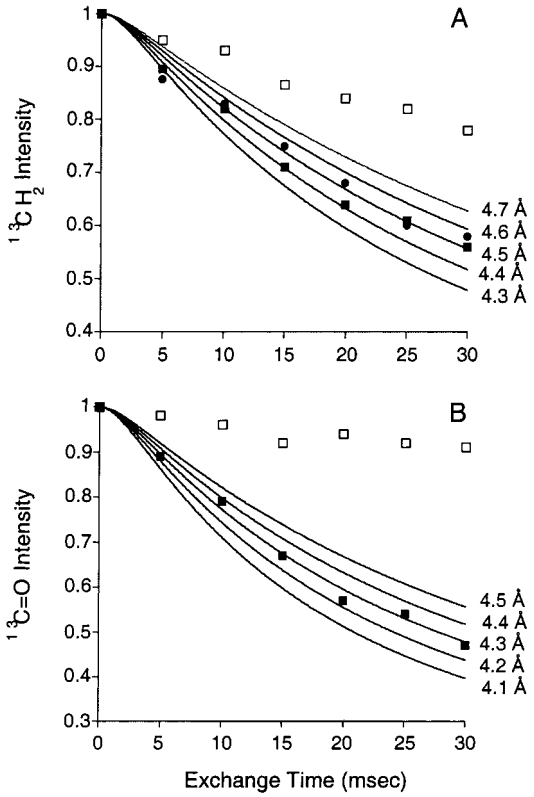

FIGURE 5: Interhelical ^{13}C rotational resonance magnetization exchange curves and simulations. (a) Experimental data are shown for the wild-type 1-^{13}C-Gly665 Neu peptide combined with 2-^{13}C-Gly665 Neu* (filled circles) and with 2-^{13}C-Gly665 Neu (open squares) peptides and for the 1-^{13}C-Gly665 Neu* peptide combined with 2-^{13}C-Gly665 Neu* (filled squares). Simulations of the magnetization exchange are shown with solid lines for internuclear distances between 4.3 and 4.7 Å using a zero quantum T_2 relaxation time of 1.4 ms. The rotational resonance data points have been corrected for off-rotational resonance decay and 29% nonexchanging 2-^{13}C-Gly labeled peptide that has formed homodimers. (b) Experimental data are shown for 2-^{13}C-Gly665 Neu* reconstituted with 1,5-^{13}C-Glu664. The MAS frequency was set to match the $n = 1$ rotational resonance condition for the 1-^{13}C-Glu664 resonance (filled squares) or the 5-^{13}C-Glu664 resonance (open squares). Simulations of the magnetization exchange are shown with solid lines for internuclear distances between 4.1 and 4.5 Å using a zero quantum T_2 relaxation time of 1.4 ms. The rotational resonance data points have been corrected for off-rotational resonance decay and 29% nonexchanging 1,5-^{13}C-Glu labeled peptide that has formed homodimers.

indicate that the peptides exist in a monomer−dimer equilibrium (*46*). Finally, recent TOXCAT measurements on the transmembrane domain of the related erbB2 receptor show that the transmembrane sequence of the wild-type receptor is able to dimerize in membranes *(3)*. Interestingly, the valine to glutamate mutation in the erbB2 transmembrane sequence did not increase the level of dimerization as it does in the Neu receptor.

Gly665−Glu664 Backbone Interactions Occur in the Neu Dimer Interface.* The absence of side chain interactions between Gln664 residues and the presence of Gly665−Gly665 interactions across the interface of the Neu* transmembrane dimer provided the motivation for distance measurements between Glu664 and Gly665. We have recently shown that both small and polar residues have a high propensity for packing in the helix interfaces of polytopic membrane proteins (*47*−*49*). Glycine does not function as a helix breaker in membrane environments but, rather, provides increased accessibility of the polar backbone atoms for interhelical hydrogen bonding interactions (*47*−*49*).

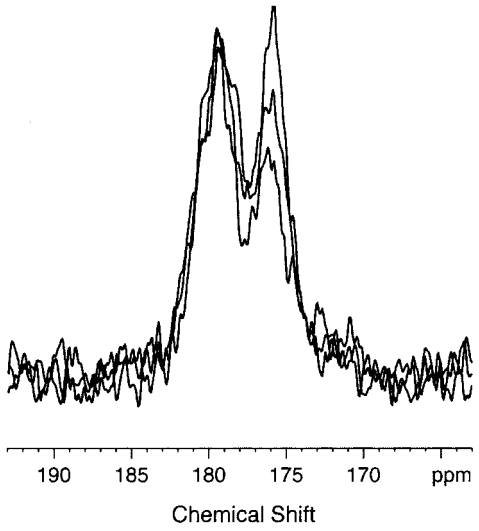

FIGURE 6: Interhelical ^{13}C rotational resonance NMR spectra of the 2-^{13}C-Gly665 Neu* transmembrane peptide reconstituted with 1,5-Glu664 Neu* peptide. The resonances are observed at 179.5 ppm (COOH) and 176.5 ppm (C═O). The MAS frequency was set to match the $n = 1$ rotational resonance condition for the 1-^{13}C-Glu664 resonance. Spectra were obtained with exchange times of 100 μs, 15 ms, and 30 ms.

In this case, glutamate was incorporated into transmembrane peptides rather than glutamine and combined with 2-^{13}C-Gly665 Neu*. The Glu664 was ^{13}C-labeled at both the backbone carbonyl and side chain carboxyl carbons. Figure 6 presents rotational resonance spectra of the carbonyl region of 1,5-^{13}C-Glu664 Neu* reconstituted with 2-^{13}C-Gly665 Neu* in a 1:4 molar ratio. There are two distinct resonances in the downfield carbonyl region of the spectrum at 179.5 and 176.5 ppm. The natural abundance ^{13}C background signal from the lipid acyl chain carbonyls has been subtracted. The resonance at 179.5 ppm is assigned to the protonated carboxyl group of Glu664 on the basis of previous experiments on 5-^{13}C-Glu664 Neu* (*27*). The MAS speed was set to equal the frequency spacing between the 2-^{13}C-Gly665 resonance and either the 1-^{13}C-Glu664 resonance (Figure 6) or the 5-^{13}C-Glu664 resonance (spectra not shown). The intensity changes in the rotational resonance experiment are plotted in Figure 5b. The dramatic change in the intensity of the backbone 1-^{13}C resonance corresponds to an interhelical 2-^{13}C-Gly665 to 1-^{13}C-Glu664 distance of 4.3 Å. In contrast, the intensity of the side chain 5-^{13}C resonance does not change significantly with longer mixing times, suggesting that the interhelical 2-^{13}C-Gly665 to 5-^{13}C-Glu664 distance is greater than ~5.5 Å. These experiments provide particularly compelling constraints since there are two similar ($^{13}C{=}O\cdots{}^{13}CH_2$) distances being compared in one sample.

Weak Gly665 Interactions Occur in the Wild-Type Neu Dimer. In this section, we address the possibility that wild-type Neu transmembrane helices may be able to interact with the activated Neu* transmembrane helices to form heterodimers or with other wild-type Neu helices to form homodimers. The dimeric state of the wild-type inactive Neu receptor in cell membranes is not known. The original model

for RTK activation postulated that the unliganded receptor exists in the monomeric state. However, more recently there has been evidence that RTKs may self-associate to form dimers even in the absence of ligand (*1*−*3*). It is known that truncation of the extracellular domain of the wild-type Neu receptor leads to dimerization and activation (*8*), demonstrating that dimer contacts form between either the transmembrane or cytoplasmic regions of the receptor. In addition, competition experiments using activated receptors and wild-type peptides indicate that strong Neu*−Neu transmembrane interactions are possible (*21*).

Figure 5a presents the rotational resonance exchange curves for the wild-type 1-^{13}C-Gly665 Neu peptide combined with 2-^{13}C-Gly665 Neu* (open circles) and with 2-^{13}C-Gly665 Neu (open squares) peptides. In these experiments, wild-type 1-^{13}C-Gly665 Neu was reconstituted with 2-^{13}C-Gly665 Neu and Neu* peptides in a 4:1 molar ratio using the same conditions as those in the experiments with Neu* alone. Comparison of the experimental and simulated exchange curves in Figure 5a shows that the exchange in the heterodimer of Neu−Neu* peptides is only slightly weaker than that in the activated Neu* homodimer but considerably stronger than that in the wild-type Neu−Neu homodimer.

There are two ways to interpret the experiments with the wild-type Neu sequence. First, the slower exchange may result from a longer internuclear distance between the 1-^{13}C and 2-^{13}C-Gly labels across the dimer interface. The exchange observed for the Neu−Neu experiment would correspond to an internuclear distance of 5−6 Å. Alternatively, the slower exchange may result from a weaker interaction between Neu peptides leading to a higher proportion of monomer. The observed exchange curve would be consistent with the 4.5 Å distance observed in the Neu* dimer if the dimer is in equilibrium with a population of ~50% monomer. The experimental data do not distinguish between these two possibilities. Interestingly, recent TOXCAT studies indicate that the efficiency of dimerization of the transmembrane domain of the wild-type human erbB2 receptor is roughly half that of human glycophorin A, which is known to form a tight dimer having a submicromolar dissociation constant (*3*).

Computational Searches of the Activated Neu Dimer Interface.* The internuclear distances obtained in the rotational resonance and REDOR experiments are clearly not sufficient to define the full three-dimensional structure of the Neu* dimer. However, both the intra- and interhelical measurements provide experimental constraints for evaluating dimer models. In this section, we describe the use of a computational search strategy developed by P. Adams and A. Brünger for locating low-energy conformations of dimers of transmembrane helices (*40*). The approach has been used to locate the dimer interface between transmembrane helices of glycophorin A (*40*). The NMR distances along with mutational data in the literature are used to evaluate probable structures which emerge from the computational searches. Once clusters of likely structures are identified, the NMR distances provide restraints for further refinement.

Figure 7 presents the results of a computational search for the Neu*−Neu* interface with Gln at position 664. Low-energy conformations of helix dimers were searched by rotating each helix relative to one another by 360° with a sampling size of 45°. The starting geometry includes both left-handed and right-handed crossing angles. Each point in the figure corresponds to a low-energy structure having either a left-handed (Figure 7a) or right-handed crossing angle (Figure 7b) between the helices. The figures show only those structures that fall into a "cluster", where a cluster is defined as a minimum of five structures with a root-mean-square deviation of 1 Å or less. These are the final minimized conformations that have migrated from their initial geometries into low-energy wells. Of the initial 512 structures in the computational search, 70 formed 9 clusters of right-handed helix dimers, and 96 formed 15 clusters of left-handed helix dimers. Three parameters make up the input for any given computational search: the peptide sequence, the sampling step size, and the helix-helix separation. The initial searches start with a step size of 45°. Simulations were run with helix separations of 9.5, 10.0, 10.5, 11.0, and 11.5 Å. The results in Figure 7 are based on a helix−helix separation of 11.0 Å. Helix−helix separations of 11.5 and 10.5 Å gave similar results.

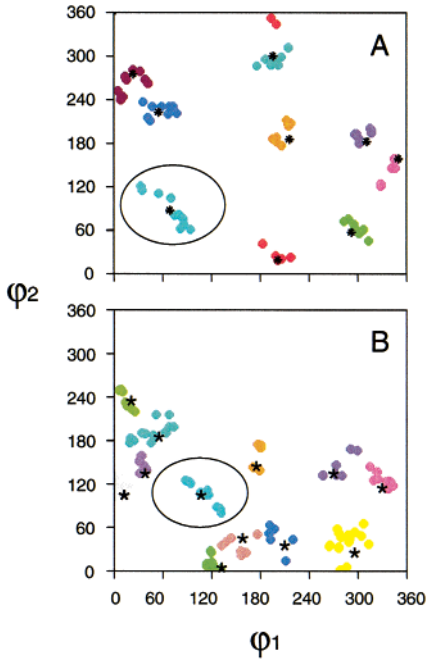

FIGURE 7: Computational search for low-energy dimer structures of the Neu* transmembrane domain. The search algorithm started with helix dimers having either left-handed (a) or right-handed (b) crossing angles. A series of molecular dynamics simulations were run after varying the angles φI and φ2, which correspond to rotation about the axes of helices 1 and 2, respectively. The step size for rotation was 45°, and four independent molecular dynamics simulations were run for each orientation. The figure plots the final φI and φ2 values for those structures that fall into a "cluster". A cluster is defined as a minimum of five structures with a root-mean-square deviation of 1 Å or less.

An average molecular structure is calculated and minimized for each cluster (marked with an asterisk) and then evaluated on the basis of constraints from the NMR measurements and mutational studies. There are two clusters (circled) that position Gly665 roughly in the dimer interface, one with a left-handed crossing angle and one with a right-handed crossing angle. The average structures from these two clusters were then minimized using the NMR distance measurements as restraints.

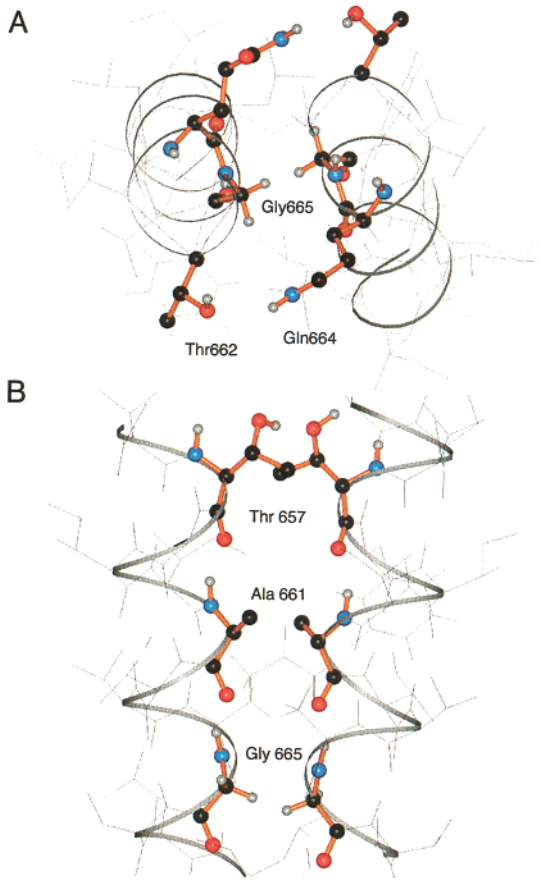

FIGURE 8: Dimer structure of the Neu* transmembrane domain derived from the computational searches and energy minimized using the NMR distance restraints. (a) View along the dimer axis. Gly665 packs in the dimer interface. Close contacts are observed between the α-carbon of Gly665 and the carbonyl carbons of Gly665 and Gln664. (b) View perpendicular to the dimer axis. The structure is a symmetric dimer with a right-handed crossing angle. Amino acids with small side chains, Gly665, Ala661, and Thr657, are predicted to line the dimer interface. The interhelical distance restraints used for the final minimization were 4.3 Å for Gly665 ($^{13}CH_2$) to Glu664 (1-^{13}C═O) and 4.5 Å for Gly665 ($^{13}CH_2$) to Gly665 (1-^{13}C═O).

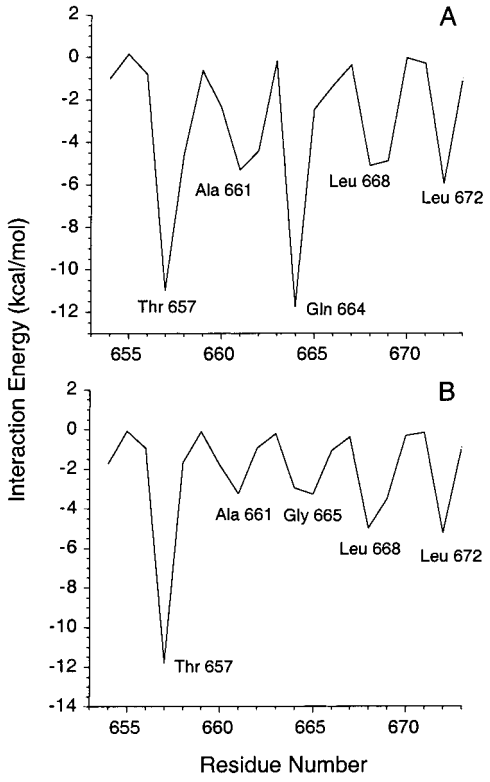

FIGURE 9: Interaction energies between transmembrane helices in the Neu* (a) and Neu (b) dimer. The energies were calculated using the program CHI. The low energies exhibited by Thr657 and Gln664 reflect interhelical hydrogen bonding.

Hydrogen Bonding and van der Waals Interactions Mediate Helix Dimerization in the Activated Neu Receptor.* Figure 8a,b shows the average low-energy structure that best fits the NMR data. The structure is a symmetric dimer with a right-handed crossing angle. Gly665 packs in the dimer interface. The packing contacts involve the α-carbon of Gly665 and the carbonyl carbons of Gln664 and Gly665. The close packing of Gly665 in the interface is consistent with the results of Stern and co-workers showing that the G665V substitution disrupted the ability of the V664E mutation to activate the receptor (*44*).

Direct Gly−Gly contacts are not unusual in membrane proteins, and the contacts in the Neu* dimer are similar to those seen in glycophorin A (*32*) and in the crystal structures of several polytopic membrane proteins (*48*). In an analysis of 158 helices in 12 polytopic membrane proteins, we have recently shown that small (Gly and Ala) and polar (Ser and Thr) residues have the highest weighted propensities for occurring in helix interfaces *(49)*. The model which emerged from these studies is that small residues allow close approach of the helix backbones and consequently facilitate interhelical hydrogen bonding of Ser and Thr side chains (*49*) and CαH···OH hydrogen bonding of the Gly residues (*48*, *51*). Gln664 does not form head-to-head hydrogen bonds but, rather, forms hydrogen bonds with the backbone carbonyl of Ala661 and the side chain of Thr662. An additional hydrogen bonding contact is predicted to form between the side chains of Thr657. Close packing of the transmembrane helices in the region of Gly665 and Ala661 may facilitate this interhelical Thr657 hydrogen bond. Additional solid-state NMR experiments are planned to characterize the hydrogen bonding interactions of Thr657 and Thr662, as well as the detailed packing of Gly665 and Ala661 in both the Neu and Neu* dimers.

Figure 9a presents calculated interaction energies for the helix dimer shown in Figure 8. The dominant contributions to dimer stability come from hydrogen bonding interactions involving Thr657, Thr662, and Gln664. In the cross-linking studies of Burke and Stern (*22*), the most significant cross links were observed for substitutions at positions 656 and 657. Both of these positions are found in the interface of the helix dimer with a right-handed crossing angle, whereas only Thr657 is found in the interface of the helix dimer identified in Figure 7a with a left-handed crossing angle and Gly665 in the dimer interface.

There are also substantial van der Waals interaction energies associated with packing of Ala661, Leu668, and Leu672. Packing of Ala661 in the interface is consistent with the intermediate phenotype observed by Cao et al. (*9*), which shows that mutation of Ala661 to isoleucine leads to a signficant reduction in the ability of the V664E mutation to transform cells. Evidence for Leu668 and Leu672 being in the interface comes from the glutamic acid replacement studies of Donoghue and co-workers (*10*).

The Neu* dimer structure provides insights into the results of Stern and co-workers (*44*), who replaced the transmembrane domain of the Neu receptor with the dimerization sequence from glycophorin A. The helix crossing angle in the glycophorin A dimer is also right-handed. Interestingly, replacing the Neu sequence with the glycophorin A sequence disrupts activation unless glutamate is present at position 664 even though the glycophorin A sequence mediates dimerization of the Neu receptor. This demonstrates that dimerization is necessary, but not sufficient, for activation (*44*). In membrane bilayers, Glu664 may shift the monomer−dimer equilibrium toward the dimer in the chimeric Neu* proteins containing the glycophorin A dimerization motif. In this regard, the stronger dipolar couplings in the Neu* dimer, in comparison to those for Neu, are consistent with higher dimerization. Alternatively, Glu664 may change the structure or orientation of the Neu* dimer.

Finally, the measured dichroic ratio of ~3.3 in polarized IR measurements on the Neu* peptides in POPC:POPS bilayers is consistent with an orientation of the helix axis of ~20° relative to the bilayer normal. This would correspond to a crossing angle between the helices of ~40°. The IR data alone do not reveal whether the helices pack with a left- or right-handed crossing angle. Helices with both left-handed and right-handed crossing angles are observed for transmembrane helices. In an analysis of polytopic membrane proteins, left-handed helices are found to be more abundant with the most common packing angle centered around +20°, whereas right-handed helices generally have a crossing angle of ~−35° (*50*, *51*). The right-handed helix crossing angle of the dimer in Figure 8 provides the best fit to the interhelical Gly−Gly and Gly−Glu constraints.

Transmembrane Helix Orientation and Rotation in the Activation of RTKs. The detailed packing of the transmembrane helices in the activated Neu* receptor containing the V664E mutation is likely to be the same as that in the ligand-activated Neu dimer. The studies of Neu receptor mutants and chimeras indicate that activation is extremely sensitive to the rotational orientation of the transmembrane helices (*10*) and the exact position of the activating mutation (*9*). The orientation and occurrence of Ala661 and Gly665 in the interface is consistent with the motif predicted by Sternberg and Gullick (*20*) for the wild-type receptor. Also, the Neu*−Neu rotational resonance experiments suggest that the same interface interacts in the wild-type Neu dimer as in the activated Neu* dimer, consistent with competition experiments using activated receptors and wild-type peptides (*21*).

Computational searches carried out for the wild-type dimer yield a number of low-energy clusters similar to those for the Neu* dimer (data not shown) with Gly665 packed in the dimer interface. Figure 9b presents the interaction energies for the lowest-energy structure of the Neu−Neu dimer that most closely matches the structure of the activated Neu* dimer. In addition to strong interhelical hydrogen bonds involving Thr657, stabilizing van der Waals interactions occur between Ala661, Gly665, Leu668, and Leu672. These interactions may be sufficient to correctly orient the transmembrane helices after ligand-binding but apparently do not stabilize the receptor dimer as effectively as the interhelical Glu664 hydrogen bonding in the Neu* dimer. As indicated above additional experiments will be needed to firmly establish whether the weak 1-^{13}C-Gly···2-^{13}C-Gly dipolar coupling, which is observed in the interhelical Neu−Neu rotational resonance experiments, results from an equilibrium involving free peptide monomers and dimers in which Gly665 is tightly packed in the dimer interface.

Table 1: Interhelical Distance Measurements in Neu*

helix 1	helix 2	interhelical distance
	REDOR	
Gln664 (5-$^{15}NH_2$)	Gln664 (5-^{13}C═O)	>6 Å
	Rotational Resonance	
Gly665 ($^{13}CH_2$)	Glu664(5-^{13}C═O)	>6 Å
Gly665 ($^{13}CH_2$)	Glu664(1-^{13}C═O)	4.3 ± 0.2 Å
Gly665 ($^{13}CH_2$)	Gly665 (1-^{13}C═O)	4.5 ± 0.2 Å

Lemmon and co-workers (*3*) recently demonstrated that the family of erbB receptors are able to self-associate in cell membranes through transmembrane interactions. The erbB2 receptor is the human homologue of the rat Neu receptor and has a similar, though not identical, transmembrane sequence. The erbB2 transmembrane domain contains two motifs which are similar to the GXXXG dimerization motif in glycophorin A. In contrast, the Neu receptor contains only the single AXXVG motif identified by Sternberg and Gullick. Using the TOXCAT system for assaying transmembrane interactions, Lemmon and co-workers (*3*) were able to show for the erbB2 receptor that both the "SAVVG" sequence in the N-terminal portion of the transmembrane domain and the "GVVFG" sequence at the C-terminal end of the transmembrane domain contribute to dimerization. Since the N-terminal dimerization sequence of the Neu receptor is involved in establishing the active orientation of the receptor, these studies suggest that the C-terminal sequence in the erbB2 receptor orients the transmembrane helices in an inactive conformation.

These observations appear to provide support for the "flexible rotation" model of Moriki et al. (*1*) for activation of the EGF (or erbB) receptor. In their model, the extracellular domain of the EGF receptor is flexible in the inactive preformed dimer, while the cytoplasmic domain is held in a rigid conformation. Upon ligand binding, a twist or rotation of the juxtamembrane (or transmembrane) region of the receptor results in increased flexibility of the cytoplasmic domain. It is possible that the position of the dimer contacts (and the helix crossing point) near the C-terminal end of the transmembrane domain helps to stabilize the inactive state of the dimer by clamping the cytoplasmic domain in an inflexible conformation. Rotation of the transmembrane helices upon ligand binding shifts the dimer contacts and helix crossing point toward the N-terminus of the transmembrane domain. This shift would increase the flexibility of the cytoplasmic domain by releasing the intracellular dimer contacts in a fashion similar to opening of a clothes pin.

ACKNOWLEDGMENT

We gratefully acknowledge the gift of 1,5-^{13}C-glutamate from the Los Alamos Stable Isotope Resource and thank Malcolm Levitt and Terry Gullion for the programs for rotational resonance and REDOR analyses, respectively, and Paul Adams and Axel Brünger for the program CHI for helix−helix analyses. We thank David Stern for many valuable discussions.

REFERENCES

1. Moriki, T., Maruyama, H., and Maruyama, I. N. (2001) Activation of preformed EGF receptor dimers by ligand-induced rotation of the transmembrane domain, *J. Mol. Biol. 311*, 1011−1026.
2. Tanner, K. G. and Kyte, J. (1999) Dimerization of the extracellular domain of the receptor for epidermal growth factor containing the membrane-spanning segment in response to treatment with epidermal growth factor, *J. Biol. Chem. 274*, 35985−35990.
3. Mendrola, J. M., Berger, M. B., King, M. C., and Lemmon, M. A. (2002) The single transmembrane domains of ErbB receptors self-associate in cell membranes, *J. Biol. Chem. 277*, 4704−4712.
4. Hubbard, S. R. (1999) Structural analysis of receptor tyrosine kinases, *Prog. Biophys. Mol. Biol. 71*, 343−358.
5. Hynes, N. E., and Stern, D. F. (1994) The biology of erbB-2/neu/HER-2 and its role in cancer, *Biochim. Biophys. Acta 1198*, 165−184.
6. Bargmann, C. I., Hung, M. C., and Weinberg, R. A. (1986) Multiple independent activations of the neu oncogene by a point mutation altering the transmembrane domain of p185, *Cell 45*, 649−657.
7. Bargmann, C. I., Hung, M. C., and Weinberg, R. A. (1986) The neu oncogene encodes an epidermal growth factor receptor-related protein, *Nature 319*, 226−230.
8. Bargmann, C. I., and Weinberg, R. A. (1988) Oncogenic activation of the neu-encoded receptor protein by point mutation and deletion, *EMBO J. 7*, 2043−2052.
9. Cao, H., Bangalore, L., Bormann, B. J., and Stern, D. F. (1992) A subdomain in the transmembrane domain is necessary for p185neu* activation, *EMBO J. 11*, 923−932.
10. Bell, C. A., Tynan, J. A., Hart, K. C., Meyer, A. N., Robertson, S. C., and Donoghue, D. J. (2000) Rotational coupling of the transmembrane and kinase domains of the Neu receptor tyrosine kinase, *Mol. Biol. Cell 11*, 3589−3599.
11. Petti, L. M., Irusta, P. M., and DiMaio, D. (1998) Oncogenic activation of the PDGF beta receptor by the transmembrane domain of p185(neu), *Oncogene 16*, 843−851.
12. Cheatham, B., Shoelson, S. E., Yamada, K., Goncalves, E., and Kahn, C. R. (1993) Substitution of the erbB-2 oncoprotein transmembrane domain activates the insulin-receptor and modulates the action of insulin and insulin-receptor substrate-1, *Proc. Natl. Acad. Sci. U.S.A. 90*, 7336−7340.
13. Wides, R. J., Zak, N. B., and Shilo, B. Z. (1990) Enhancement of tyrosine kinase-activity of the Drosophila epidermal growth-factor receptor homologue by alterations of the transmembrane domain, *Eur. J. Biochem. 189*, 637−645.
14. Yarden, Y., and Schlessinger, J. (1987) Self-phosphorylation of epidermal growth-factor receptor - evidence for a model of intermolecular allosteric activation, *Biochemistry 26*, 1434−1442.
15. Matsushime, H., Wang, L. H., and Shibuya, M. (1986) Human C-Ros-1 gene homologous to the v-ros sequence of ur2 sarcoma-virus encodes for a transmembrane receptor-like molecule, *Mol. Cell. Biol. 6*, 3000−3004.
16. Martinzanca, D., Hughes, S. H., and Barbacid, M. (1986) A human oncogene formed by the fusion of truncated tropomyosin and protein tyrosine kinase sequences, *Nature 319*, 743−748.
17. Downward, J., Yarden, Y., Mayes, E., Scrace, G., Totty, N., Stockwell, P., Ullrich, A., Schlessinger, J., and Waterfield, M. D. (1984) Close similarity of epidermal growth-factor receptor and v-erb- b oncogene protein sequences, *Nature 307*, 521−527.
18. Giordano, S., Direnzo, M. F., Narsimhan, R. P., Cooper, C. S., Rosa, C., and Comoglio, P. M. (1989) Biosynthesis of the protein encoded by the c-met proto-oncogene, *Oncogene 4*, 1383−1388.
19. Takahashi, M., and Cooper, G. M. (1987) Ret transforming gene encodes a fusion protein homologous to tyrosine kinases, *Mol. Cell. Biol. 7*, 1378−1385.
20. Sternberg, M. J., and Gullick, W. J. (1990) A sequence motif in the transmembrane region of growth factor receptors with tyrosine kinase activity mediates dimerization, *Protein Eng. 3*, 245−248.
21. Lofts, F. J., Hurst, H. C., Sternberg, M. J., and Gullick, W. J. (1993) Specific short transmembrane sequences can inhibit transformation by the mutant neu growth factor receptor in vitro and in vivo, *Oncogene 8*, 2813−2820.
22. Burke, C. L., and Stern, D. F. (1998) Activation of Neu (ErbB-2) mediated by disulfide bond-induced dimerization reveals a receptor tyrosine kinase dimer interface, *Mol. Cell. Biol. 18*, 5371−5379.
23. Sajot, N., and Genest, M. (2000) Structure prediction of the dimeric neu/ErbB-2 transmembrane domain from multi-nanosecond molecular dynamics simulations, *Eur. Biophys. J. Biophys. Lett. 28*, 648−662.
24. Smith, S. O., Aschheim, K., and Groesbeek, M. (1996) Magic angle spinning NMR spectroscopy of membrane proteins, *Q. Rev. Biophys. 29*, 395−449.
25. Griffiths, J. M., and Griffin, R. G. (1993) Nuclear magnetic resonance methods for measuring dipolar couplings in rotating solids, *Anal. Chim. Acta 283*, 1081−1101.
26. Zhao, X., Eden, M., and Levitt, M. H. (2001) Recoupling of heteronuclear dipolar interactions in solid-state NMR using symmetry-based pulse sequences, *Chem. Phys. Lett. 342*, 353−361.
27. Smith, S. O., Smith, C. S., and Bormann, B. J. (1996) Strong hydrogen bonding interactions involving a buried glutamic acid in the transmembrane sequence of the neu/erbB-2 receptor, *Nat. Struct. Biol. 3*, 252−258.
28. Peersen, O. B. (1994) Rotational resonance NMR of crystalline and membrane bound peptides, Ph.D. Thesis, Yale University, New Haven, CT.
29. Raleigh, D. P., Levitt, M. H., and Griffin, R. G. (1988) Rotational resonance in solid state NMR, *Chem. Phys. Lett. 146*, 71−76.
30. Peersen, O. B., Groesbeek, M., Aimoto, S., and Smith, S. O. (1995) Analysis of rotational resonance magnetization exchange curves from crystalline peptides, *J. Am. Chem. Soc. 117*, 7228−7237.
31. Gullion, T., and Schaefer, J. (1989) Rotational-echo double-resonance NMR, *J. Magn. Reson. 81*, 196−200.
32. Smith, S. O., Song, D., Shekar, S., Groesbeek, M., Ziliox, M., and Aimoto, S. (2001) Structure of the transmembrane dimer interface of glycophorin A in membrane bilayers, *Biochemistry 40*, 6553−6558.
33. Bechinger, B., Ruysschaert, J. M., and Goormaghtigh, E. (1999) Membrane helix orientation from linear dichroism of infrared attenuated total reflection spectra, *Biophys. J. 76*, 552−563.
34. Smith, S. O., Eilers, M., Song, D., Crocker, E., Ying, W., Groesbeek, M., Metz, G., Ziliox, M., and Aimoto, S. (2002) Implications of threonine hydrogen bonding in the glycophorin A transmembrane helix dimer, *Biophysical J., in press*.
35. Metz, G., Wu, X., and Smith, S. O. (1994) Ramped-amplitude cross polarization in magic angle spinning NMR, *J. Magn. Reson. A 110*, 219−227.
36. Bennett, A. E., Rienstra, C. M., Auger, M., Lakshmi, K. V., and Griffin, R. G. (1995) Heteronuclear decoupling in rotating solids, *J. Chem. Phys. 103*, 6951−6958.
37. Metz, G., Ziliox, M., and Smith, S. O. (1996) Towards quantitative CP-MAS NMR, *Solid-State NMR 7*, 155−160.
38. Levitt, M. H., Raleigh, D. P., Creuzet, F., and Griffin, R. G. (1990) Theory and simulations of homonuclear spin pair systems in rotating solids, *J. Chem. Phys. 92*, 6347−6364.
39. Gullion, T., and Schaefer, J. (1991) Elimination of resonance offset effects in rotational-echo, double-resonance NMR, *J. Magn. Reson. 92*, 439−442.
40. Adams, P. D., Engelman, D. M., and Brunger, A. T. (1996) Improved prediction for the structure of the dimeric transmembrane domain of glycophorin A obtained through global searching, *Proteins 26*, 257−261.
41. Adams, P. D., Arkin, I. T., Engelman, D. M., and Brunger, A. T. (1995) Computational searching and mutagenesis suggest a structure for the pentameric transmembrane domain of phospholamban [see comments], *Nat. Struct. Biol. 2*, 154−162.
42. Brandt-Rauf, P. W., Rackovsky, S., and Pincus, M. R. (1990) Correlation of the structure of the transmembrane domain of the neu oncogene-encoded p185 protein with its function, *Proc. Natl. Acad. Sci. U.S.A. 87*, 8660−8664.
43. Gratkowski, H., Lear, J. D., and DeGrado, W. F. (2001) Polar side chains drive the association of model transmembrane peptides, *Proc. Natl. Acad. Sci. U.S.A. 98*, 880−885.
44. Burke, C. L., Lemmon, M. A., Coren, B. A., Engelman, D. M., and Stern, D. F. (1997) Dimerization of the p185neu transmembrane domain is necessary but not sufficient for transformation, *Oncogene 14*, 687−696.
45. Oka, T., Kamikubo, H., Tokunaga, F., Lanyi, J. K., Needleman, R., and Kataoka, M. (1999) Conformational change of helix G in the bacteriorhodopsin photocycle: Investigation with heavy atom labeling and X-ray diffraction, *Biophys. J. 76*, 1018−1023.

46. Sharpe, S., Barber, K. R., and Grant, C. W. M. (2000) Val(659)→Glu mutation within the transmembrane domain of ErbB-2: Effects measured by ^{2}H NMR in fluid phospholipid bilayers, *Biochemistry 39*, 6572−6580.
47. Eilers, M., Shekar, S. C., Shieh, T., Smith, S. O., and Fleming P. J. 2000. Internal packing of helical membrane proteins, *Proc. Natl. Acad. Sci. U.S.A. 97*, 5796−5801
48. Javadpour, M. M., Eilers, M., Groesbeek, M., and Smith, S. O. (1999) Helix packing in polytopic membrane proteins: role of glycine in transmembrane helix association, *Biophys. J. 77*, 1609−1618.
49. Eilers, M, Patel, A., Liu, W., and Smith, S. O. (2002) Comparison of helix interactions in membrane and soluble proteins, *Biophysical J. 82*, 2720−2736.
50. Bowie, J. U. (1997) Helix packing in membrane proteins, *J. Mol. Biol. 272*, 780−789.
51. Senes, A., Ubarretxena-Belandia, I., and Engelman, D. M. (2001) The Cα-H...O hydrogen bond: A determinant of stability and specificity in transmembrane helix interactions, *Proc. Natl. Acad. Sci. U.S.A. 98*, 9056−9061.

BI012117L